



## INTERNATIONAL JOURNAL OF ENGINEERING SCIENCES & RESEARCH TECHNOLOGY

### A Novel Approach towards Gas Sensing Through A.C.Conductivity of Tin Oxide- Aluminum Oxide Composite

Alison Christina Fernandez, P.Sakthivel, Joe Jesudurai\*

\*Department of Physics, Loyola College, Chennai 600034, Tamil Nadu, India

[joejesudurai@gmail.com](mailto:joejesudurai@gmail.com)

#### Abstract

The present paper reports the synthesis of SnO-Al<sub>2</sub>O<sub>3</sub> composites via the hydrothermal route. The as-synthesized materials are characterized by different techniques, such as X-ray diffraction, High resolution scanning electron microscopy and UV-Visible spectroscopy. The A.C.conductivity of the composites were determined in the ambient and cigarette smoke environment. The results show that the composites are potentially suitable candidates for sensing application.

**Keywords:** Cigarette smoke; A.C.Conductivity; X-ray diffraction analysis; hydrothermal; composite.

#### Introduction

There always exists burgeoning interests in the field of semiconductor materials and its applications. Semiconductor oxides are widely used as sensors to detect leaks both in the domestic and industrial areas. Tin oxide, among the semiconductors, is the most sought after metal oxide because of its chemical stability and high sensitivity at low operating temperatures [1]. SnO and SnO<sub>2</sub> are the two important forms of tin oxide, among its various binary and ternary forms. Tin monoxide (SnO) is a wide, indirect band gap, p-type semiconductor which has received much attention due to its technological significance. It has been analyzed and applied for various applications such as lithium batteries [2, 3], gas sensors [4, 5], catalysts for several acids and coating materials [6-8]. Aluminum oxide exists in a wide range of polymorphs [9]. They are particularly important materials used as catalysts, absorbents, nanocomposite fillers, high performance ceramics and many other applications [10]. Alumina has also many interesting properties such as high hardness, stability, insulation and also good transparency [11]. Researchers, of late, are showing immense interest in the synthesis of aluminum oxide and its composites, because of its important and diverse properties and significant applications [12-14].

Tobacco smoking is prevalent worldwide and from statistics the numbers have reached over a thousand million people. Tobacco is commonly smoked as cigarettes, which is known to be a sophisticated nicotine delivery system [15]. There are over 4000 chemicals in tobacco smoke, nicotine

being the drug which causes the addiction in smokers. Besides nicotine, there is also carbon monoxide and tar present, which are the next highly toxic elements. Researchers advocate that the damage done to passive smokers have been underestimated. In recent findings it is observed that around 30,000 deaths from heart attacks are due to passive smoking [16].

In the present work, the tin-aluminum oxide composites were synthesized hydrothermally. X-ray diffraction, UV-Vis spectrometry, SEM and dielectric analysis were employed in order to characterize the produced composite powders. The X-ray diffraction was used to analyze the microstructural details of the composites. The influence of the variation in molar ratios on the crystallite size and lattice strain has been reported. The novelty of this work was to investigate the electrical response of the oxides-composites to cigarette smoke which would be an efficient way to improve sensor performance.

#### Experimental

All the chemicals obtained were of analytical grade and used as received without purification. Tin chloride dehydrate (SnCl<sub>2</sub>.2H<sub>2</sub>O, 97%), Aluminum nitrate (Al(NO<sub>3</sub>)<sub>3</sub>.9H<sub>2</sub>O, 98%) and Urea ((NH<sub>2</sub>)<sub>2</sub>CO, 99.5%) were used as starting materials. The synthesis procedure was carried out as follows. Tin chloride was dissolved in 150ml of de-ionised water and stirred well to yield a solution. Next Aluminum nitrate was added to the solution. Finally 0.2M of urea was added to the above solution and stirred for an hour before loading it into a Teflon lined autoclave. The precursor solution was then treated

hydrothermally at 180°C for 2 hours. The obtained composite was washed multiple times with water and acetone thoroughly. It was annealed at 200°C for 2 hours. The finely powdered sample was then subjected to various characterisations.

The above procedure was followed for 3 different molar ratios [0.5:0.5], [0.25:0.75] and [0.75:0.25] of the tin and aluminum precursors.

An X-ray diffractometer (XRD) was used to study the crystalline phase structure of all the composites. The samples were scanned between 20° and 70° with CuK $\alpha$  (1.5406Å) radiation using the Seifert 3003T/T X-ray diffractometer. Scanning electron microscopy (SEM) and Energy dispersive spectroscopy (EDAX) were performed using a FEI Quanta FEG 200 Scanning Electron microscope equipped with an EDAX detector. A Ultra-violet visible (UV-Vis) Lambda 35 spectrophotometer in a range of 200 to 1100nm was used to study the optical absorption. The optical band gap was determined by

analysing the data obtained. The electrical properties of the sample with respect to the cigarette smoke was measured by the Hitachi 3532-50 LCR Hitester.

### Results and discussion

Figure 1 shows the typical XRD patterns of the composites of tin oxide-aluminum oxide with different Sn/Al ratios. All the diffraction peaks match well with those of the standard SnO XRD pattern [JCPDS card file no.: 06-0395] and are attributed to the tetragonal phase. Moreover no characteristic diffraction peaks from aluminium were observed. This can be attributed to its highly amorphous phase in the composite [17]. Thereby it also proves that the crystalline nature of SnO is formed by the hydrothermal synthesis. However the SEM-EDAX elemental analysis for the Sn-Al sample was carried out and the analysis confirmed the presence of aluminum in all the three molar ratios (figure 4).

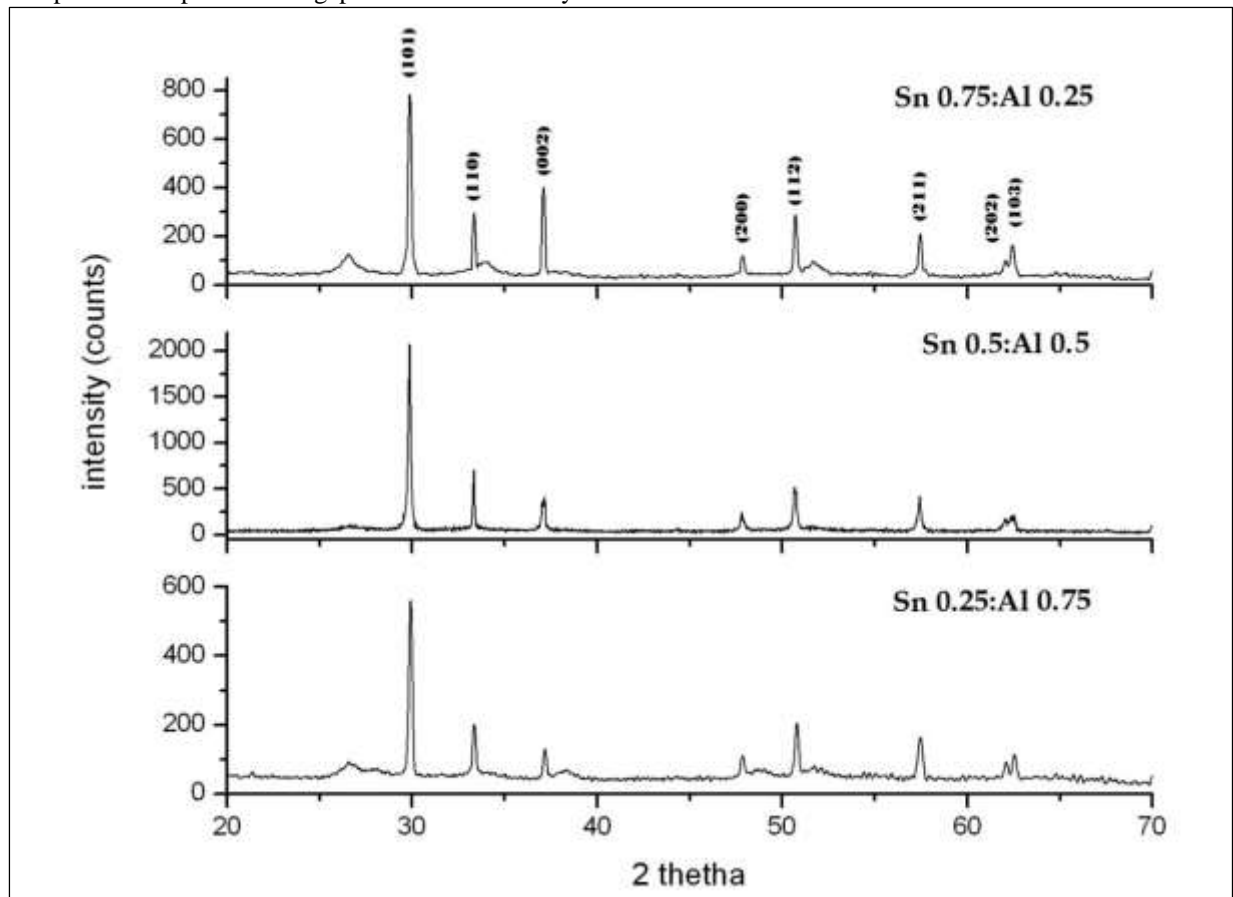


**Figure 1: XRD patterns of the as-prepared SnO – Al<sub>2</sub>O<sub>3</sub> composite particles annealed at 200°C were initially synthesized using 3 different molar ratios**

The lattice parameters of SnO are thereby calculated and tabulated (Table 1). The crystallite size of the material was estimated by the Scherrer's equation

$$d = \frac{k\lambda}{\beta \cos\theta}$$

Where  $\beta$  is the full width at half maximum (FWHM) of the observed peak,  $k$  is the Scherrer's constant,  $\lambda$  is

the X-ray wave length for CuK $\alpha$  radiation (1.5406 Å),  $\theta$  is the Bragg diffraction angle.

The FWHM of the reflected XRD peak was also used to estimate the lattice strain by assuming that the strain and the crystallite size are dependent on the line broadening. The microstrain is thereby calculated by using the equation

$$\epsilon_{str} = \beta / 4 \tan \theta$$

Dislocation density is the length of the dislocation lines per unit volume. Its presence is known to have a strong impact on the properties of the material. Literature reveals that the dislocation density and the

microstrain increases as the grain size decreases [18]. The dislocation density  $\delta$  of the given composite was estimated by the formula

$$\delta = \frac{15\epsilon}{ad}$$

It was observed from the tabulated data (Table 1) that the dislocation density was found to be inversely proportional to the crystallite size. Figure 2 and 3 represent the variation of the crystallite size and strain with respect to the varying molar ratios of the composite.

SnO[06-0395]	SnO[0.75]:Al <sub>2</sub> O <sub>3</sub> [0.25]	SnO[0.5]:Al <sub>2</sub> O <sub>3</sub> [0.5]	SnO[0.25]:Al <sub>2</sub> O <sub>3</sub> [0.75]
$a = b = 3.802$ [Å]	$3.803 \pm 0.012$	$3.808 \pm 0.016$	$3.798 \pm 0.006$
$c = 4.836$ [Å]	$4.838 \pm 0.015$	$4.849 \pm 0.022$	$4.835 \pm 0.006$
$V = 69.91$ [Å <sup>3</sup> ]	69.98	70.33	69.74
Crystallite size [101] (nm)	41.38	61.01	41.11
Microstrain[101]	$3.402 \times 10^{-3}$	$2.314 \times 10^{-3}$	$3.414 \times 10^{-3}$
Dislocation density[101] (lines/m <sup>2</sup> )	$3.24 \times 10^{15}$	$1.49 \times 10^{15}$	$3.28 \times 10^{15}$

Table 1: Lattice constants calculated for the distinct SnO peaks for the 3 molar ratios.

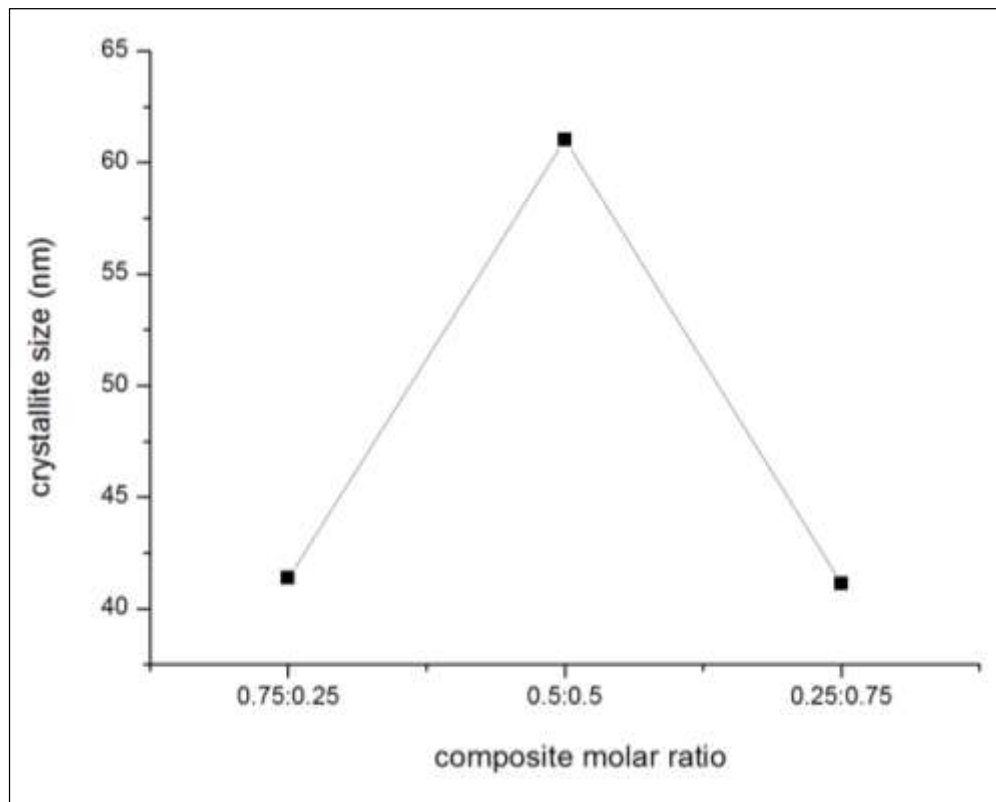


Figure 2: Variation of the crystallite size with the molar ratios of the precursors

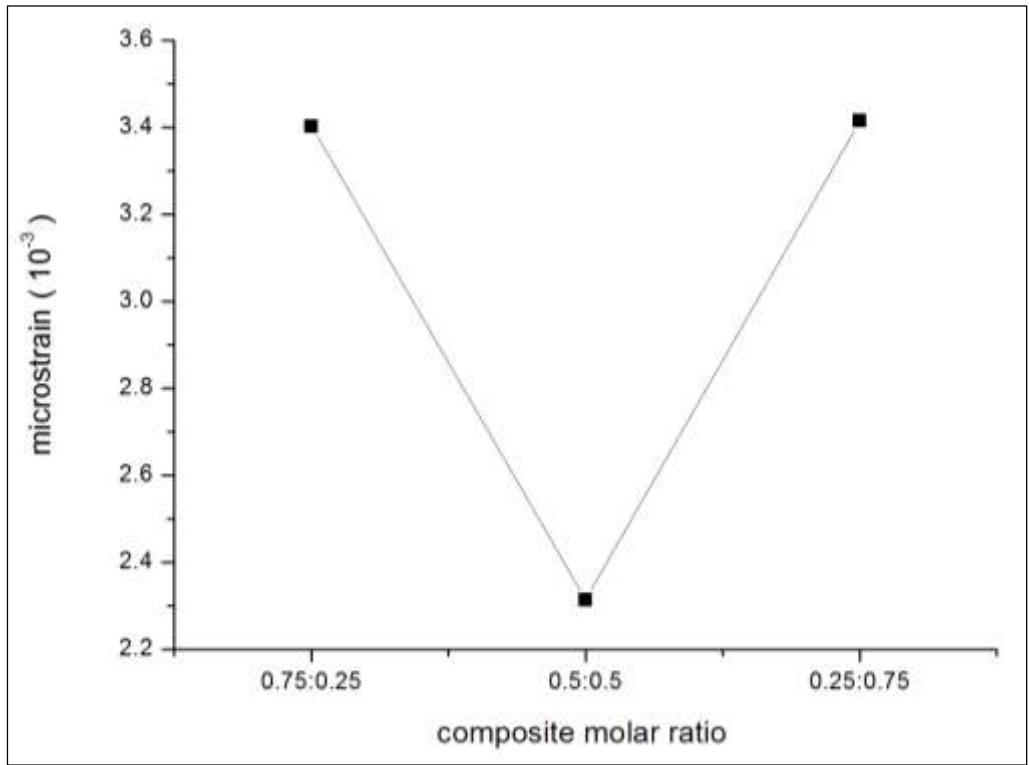


Figure 3: Variation of the microstrain with the molar ratios of the precursors

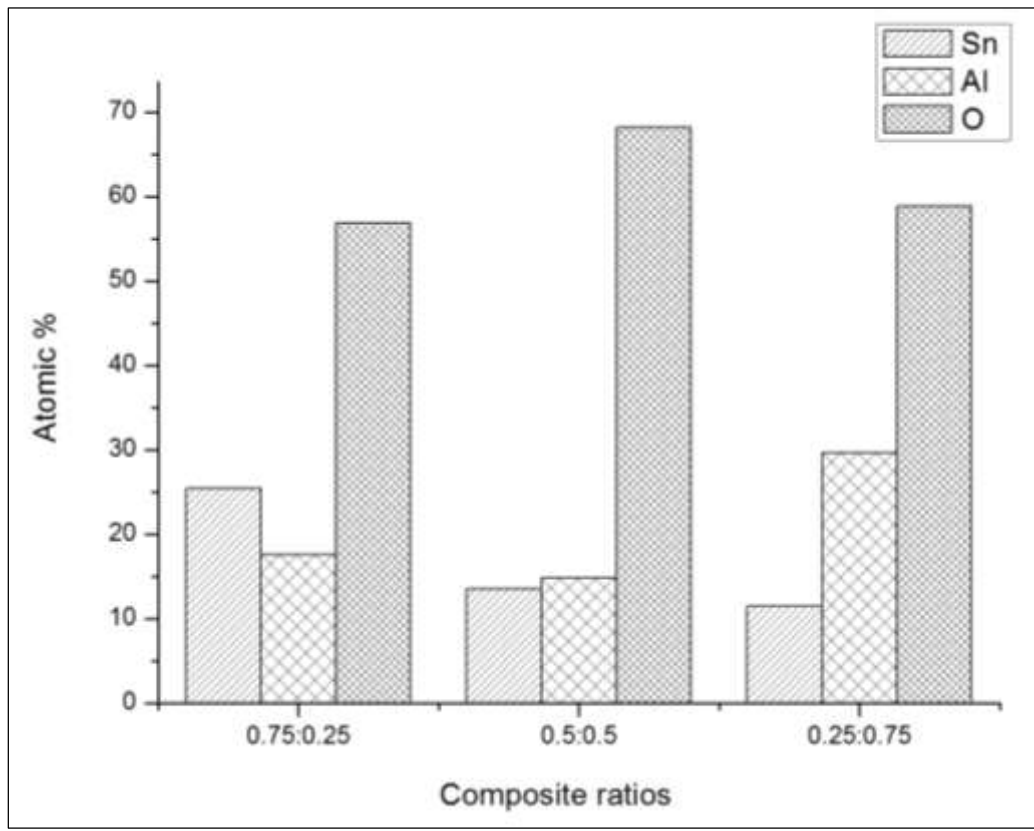


Figure 4: Graphical comparison of the Atomic % of the elements present in the 3 synthesized composites obtained by the EDX analysis

Sample	Std	Cal	BG Difference		
			BG (eV)	$\lambda$ (nm)	BG (eV)
SnO	0.75	316.72	3.93	0.93	41.11
	0.5	339.21	3.67	0.67	61.07
	0.25	326.36	3.81	0.81	41.38
Al <sub>2</sub> O <sub>3</sub>	0.25	7.4	Below the wavelength of measurement		
	0.5				
	0.75				

*Table 2: Tabulation of the observed excitation wavelengths and the comparison between the bulk and calculated band gaps of SnO and Al<sub>2</sub>O<sub>3</sub> for the different molar ratios.*

SnO with its four coordinate square pyramidal tin atoms [19] is known to have an electronic band gap between 2.5 – 3 eV [20]. The electrical band gap otherwise known as transport band gap, is the threshold for creating an electron-hole pair that is not bound together. In most inorganic semiconductors, the optical and electronic band gaps are fundamentally identical. The UV-Vis absorption spectra data of the composites are tabulated in table 2. A blue shift of the band gap is observed compared to

the bulk material in all three cases. It is also observed that the band gap increases with the decrease in the crystallite size.

The micro-structure of the composite samples annealed at 200°C investigated by FESEM are shown in figures 5a,5b and 5c. The SEM photographs at high magnification reveal a flake-like morphology in all three cases.

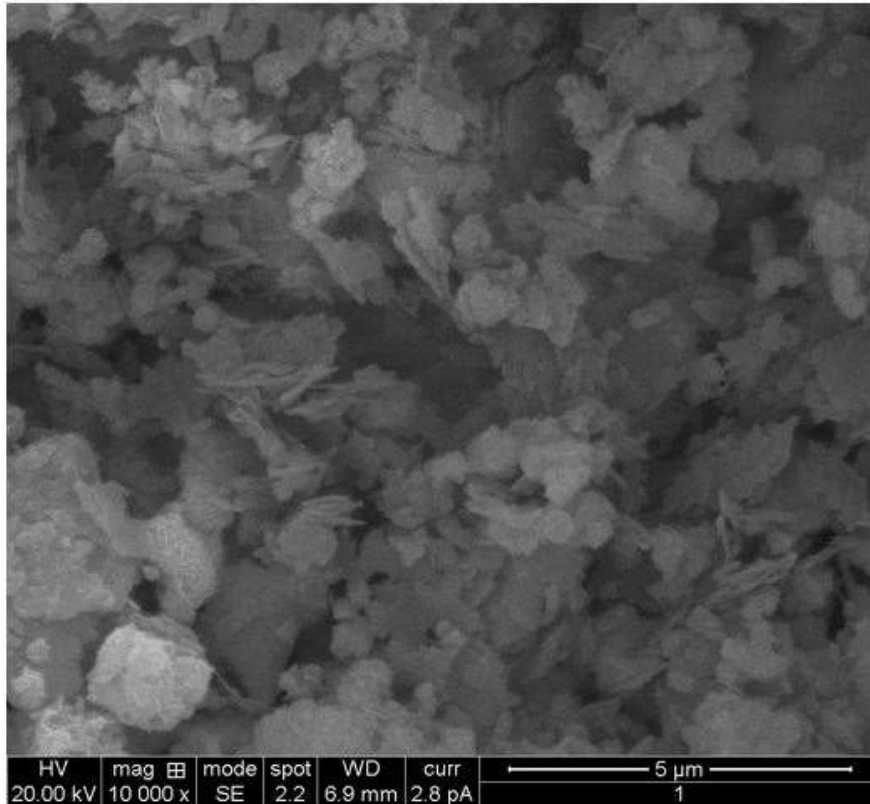


*Figure 5a:HRSEM morphology for the SnO-Al<sub>2</sub>O<sub>3</sub> composite with molar ratio 0.75:0.25*



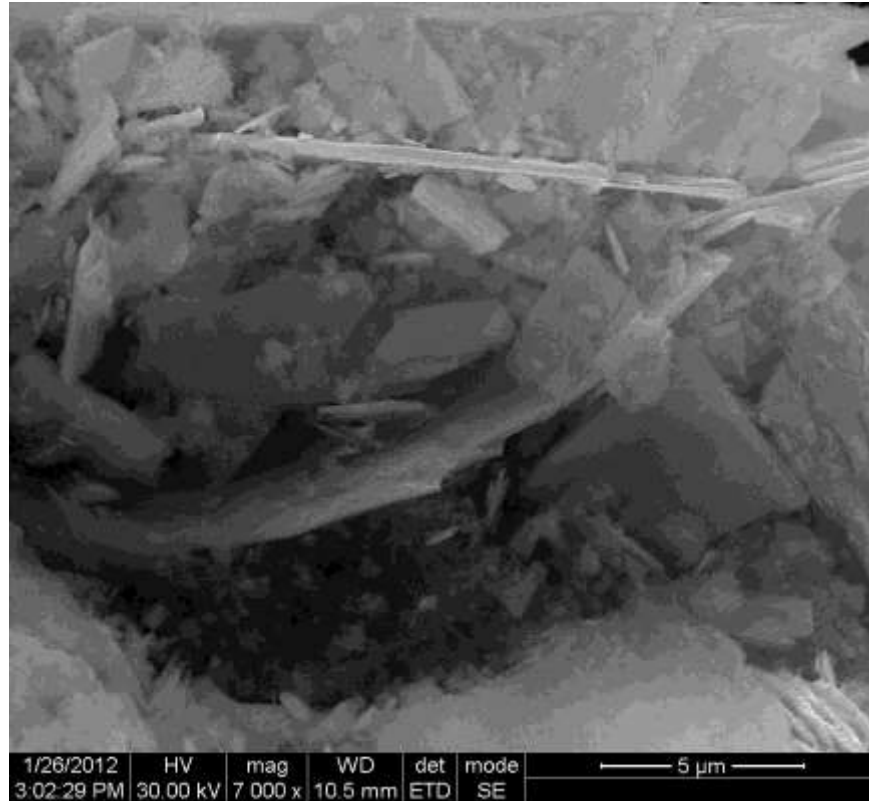


Figure 5b: HRSEM morphology for the SnO-Al<sub>2</sub>O<sub>3</sub> composite with molar ratio 0.5:0.5

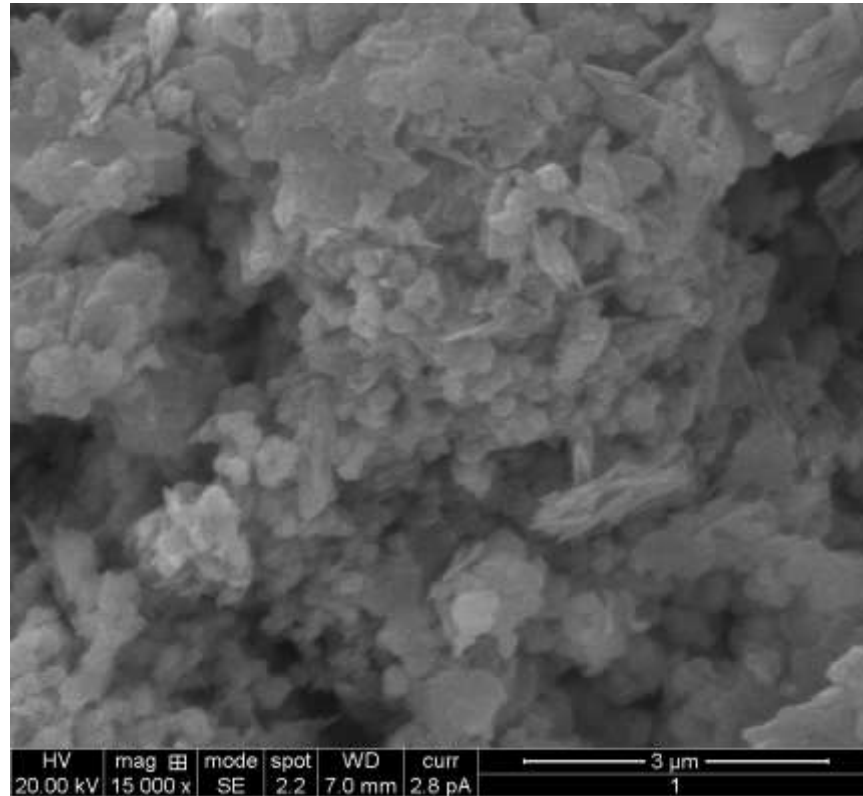


Figure 5c: HRSEM morphology for the SnO-Al<sub>2</sub>O<sub>3</sub> composite with molar ratio 0.25:0.75

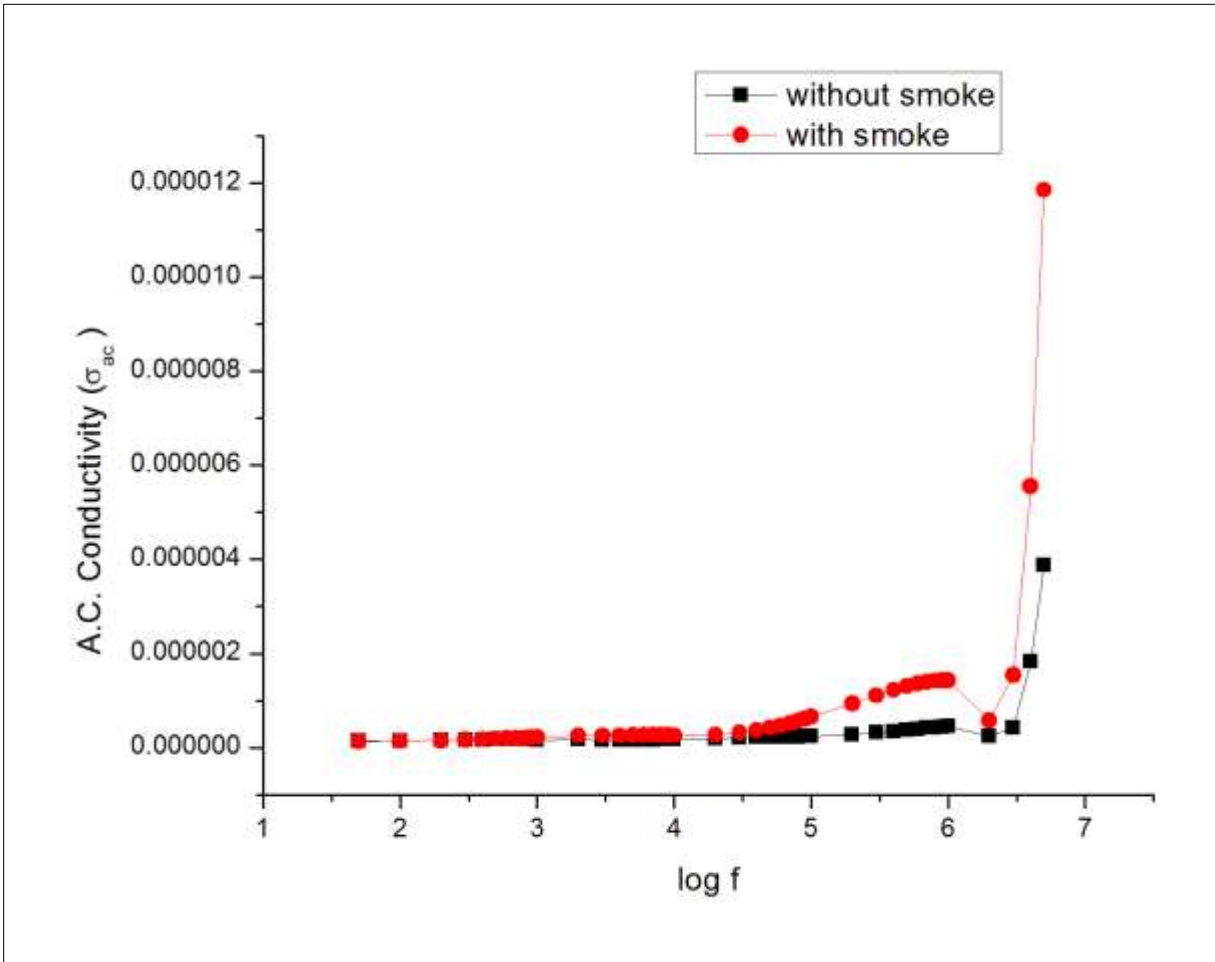


Figure 6a: Plot of A.C. conductivity for the 0.75:0.25 ratio of the SnO-Al<sub>2</sub>O<sub>3</sub> composite

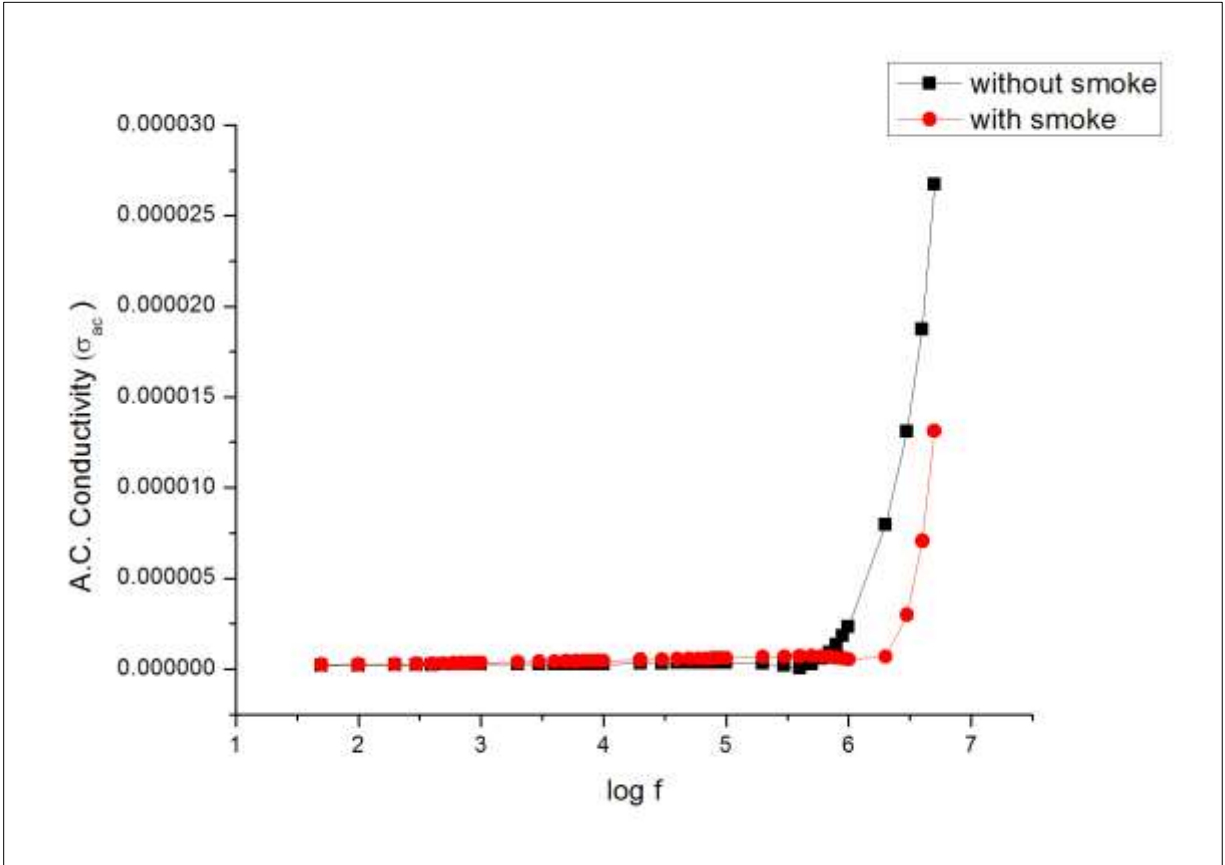


Figure 6b: Plot of A.C. conductivity for the 0.5:0.5 ratio of the SnO-Al<sub>2</sub>O<sub>3</sub> composite



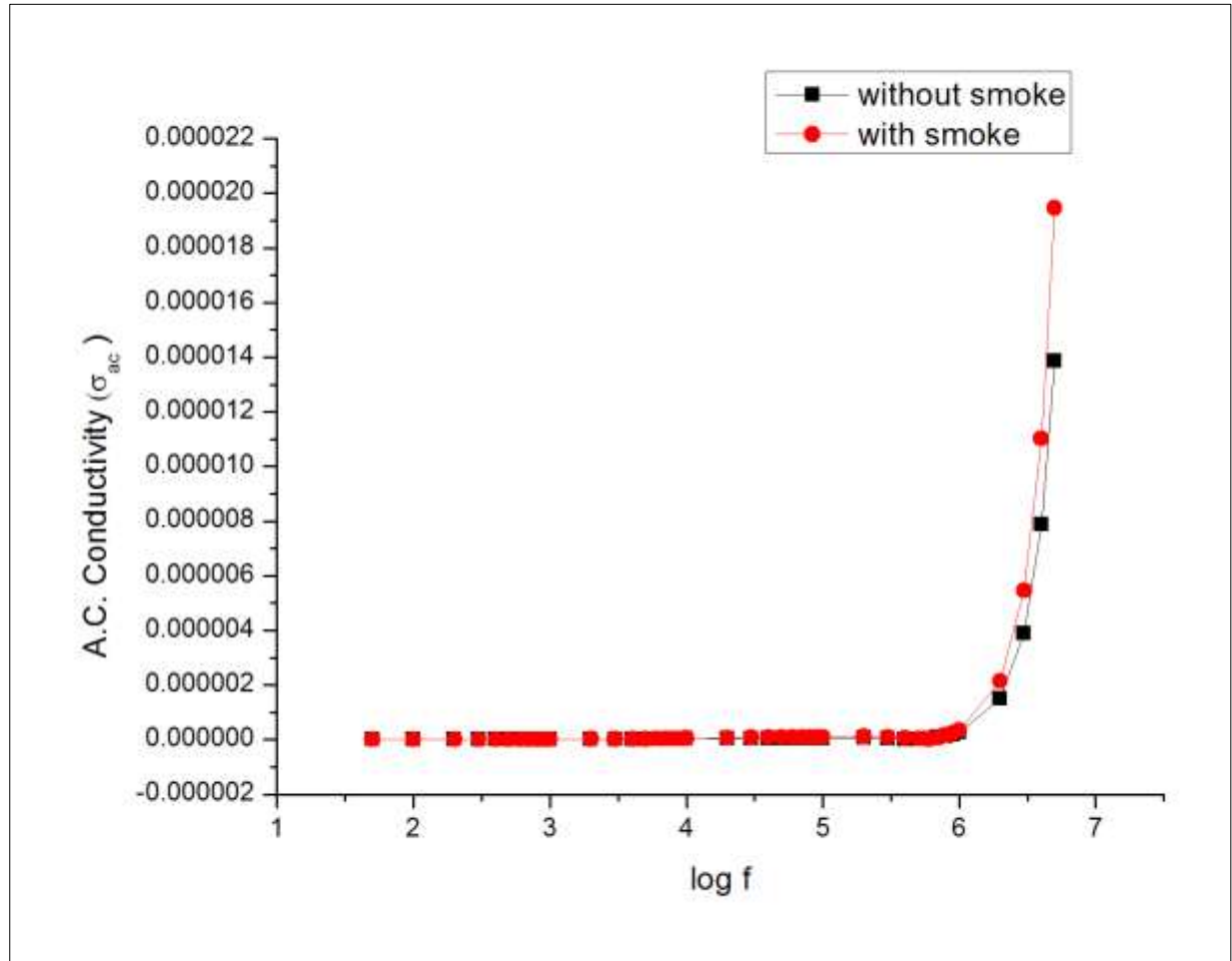


Figure 6c: Plot of A.C. conductivity for the 0.25:0.75 ratio of the SnO-Al<sub>2</sub>O<sub>3</sub> composite

Second hand smoking is formed when cigarettes and other tobacco products are burnt and also from the smoke exhaled from the smoker. This exposure is often termed as passive/ involuntary smoking. The mainstream smoke is primarily composed of carbon monoxide, particles and nicotine at varying percentages, but over 7000 additional constituents have also been identified and reported [21]. These substances and particles travel deep into the lungs causing immunological damage and are also known to cause cancers in humans. Literature reveals that exposure to SHS is more harmful to non-smokers, especially children.

There is no known or suspected mechanism by which active smoking would protect an individual against the effects of passive smoking. Monitoring smoking in indoor spaces and commonly used public areas is the only way non-smokers can be protected from second-hand-smoke exposure.

The A.C. conductivity of the composites was studied by converting the as-prepared samples into pellets under a pressure of 10 tonnes and subjecting them to

an alternating voltage. The response of the samples in ambient and cigarette smoke environment was studied using a dielectric analyzer.

The A.C. conductivity is calculated using the formula  $\sigma_{ac} = 2\pi f \epsilon_0 \epsilon_r \tan \delta$ ,

Where  $\epsilon_0 = 8.854 \times 10^{-12}$  F/m,  $\epsilon_r$  is the dielectric constant and  $\tan \delta$  is the dielectric loss. It is primarily observed that metal oxides exhibit a change in conductivity occurring due the adsorption of the molecules from the gas phase with the surface of the material. The fundamental principle behind this is that the target gas interacts with the surface of the metal oxide (through the surface adsorbed oxygen ions) resulting in a change in the charge carrier concentration. This change serves to alter the conductivity of the material.

The figures 6(a), (b) and (c) graphically represent the A.C. conductivity of the composites at room temperature. It is observed that as the frequency of the applied voltage increases the A.C. conductivity ( $\sigma_{ac}$ ) increases. There is also an increase in the

A.C. conductivity of all the three composites when the smoke is introduced. Percentage of change in A.C. conductivity due to cigarette smoke was calculated using the formula

$$\% \sigma_{AC} = \frac{\text{Diff } \sigma_{AC}}{\text{Air } \sigma_{AC}} \times 100$$

The values were calculated at 5MHz and are tabulated below (Table 3).

SnO:Al <sub>2</sub> O <sub>3</sub>	[0.75:.25]	[0.5:0.5]	[0.25:0.75]
% Change in $\sigma_{ac}$ due to cigarette smoke	66.69	50.48	28.16

Table 3: Percentage change in A.C. conductivity value due to cigarette smoke of the composites

## Conclusion

Composites of tin oxide-alumina with flake-like morphology have been successfully synthesized via a facile hydrothermal process by varying the molar ratios of the precursors of tin and aluminum. According to XRD analysis, the annealed powders consist of a single phase of SnO without any visible peaks of alumina due to its existence in the amorphous form. Further calculations like crystallite size, lattice strain and dislocation density were also reported. From the UV-Visible analysis, the value of the band gap was determined. The A.C. conductivity of the materials was measured in the presence of air and cigarette smoke. The composites presented a good response to the cigarette smoke, implying that the composite and the technique used can open up novel ways of gas sensing and device fabrication.

## Reference

1. Kiran Jain Rashmi, S.T.Lakshmikummar, Preparation of nanocrystalline tin oxide powder for gas sensor applications, *J.Surface Sci. Tech.*, Vol 21, No 3-4 (2005), pp 129-138
2. Y. Idota, A. Matsufuji, Y. Mackawa, T. Miyasaka, Tin-Based Amorphous Oxide: A High-Capacity Lithium-Ion-Storage Material, *Mater. Sci.*, Vol. 276, (1997), pp.1395-1397.
3. I. A.Courtney, J.R. Dahn, *Electrochemical and In Situ X-Ray Diffraction Studies of the Reaction of Lithium with Tin Oxide Composites*, *J. Electrochem Soc.*, Vol.144, (1997), pp. 2045-2052.
4. S.G. Ansari, S.K. Kulkarni, R.N. Karekar, R.C.Aiyer, Effect of thickness on H<sub>2</sub> gas sensitivity of SnO<sub>2</sub> nanoparticle-based thick film resistors, *J. Mat. Sci.Mater. Electr.*, Vol. 7, (1996), pp. 267-270.
5. S.G. Ansari, P. Boroojerdian, S.R. Sainkar, R.C.Aiyer, S.K. Kulkarni, Grain size effects on H<sub>2</sub> gas sensitivity of thick film resistor using SnO<sub>2</sub> nanoparticles, *Thin Solid Films*, Vol. 295, (1997), 271-276.
6. Z. Han, N.Guo, F. Li, W. Zhang, H. Zhao, Y. Quian, Solvothermal preparation and morphological evolution of stannous oxide powders, *Mater. Lett.*, Vol. 48, (2001), pp. 99-103
7. O. Mao, R.L. Turner, I.A. Courtney, B.D. Fredericksen, M.I. Buckett, L.J. Krause, Active/Inactive Nanocomposites as Anodes for Li-Ion Batteries, *Electrochem. Solid-State Lett.*, Vol. 2, (1999), pp. 3-5.
8. N. Li, C. Martin, A High-Rate, High-Capacity, Nanostructured Sn-Based Anode Prepared Using Sol-Gel Template Synthesis, *J. Electrochem. Soc.*, Vol. 148, (2001), pp. A164-170.
9. O.V.Al'myasheva, E.N.Korytkova, A.V.Maslov, V.V.Gusarov, Preparation of Nanocrystalline Alumina under Hydrothermal Conditions, *Inorganic Materials*, Vol. 41, No. 5, 2005, pp. 460-467
10. Shuxue Zhou, Markus Antonietti, Markus Niaderberger, Low temperature synthesis of  $\gamma$ -alumina nanocrystals from aluminum acetylacetonate in non aqueous media, *small* 2007, 3, nos 763-767
11. L.D.Hart, *Alumina chemicals : science and technology handbook*, American Ceramic Society, Ohio, US 1990
12. Kobayashi Y, Ishizaki T, Kurokawa Y, Preparation of alumina films by sol-gel method, *J.Mater.Sci* 2005, 40 (2) 263-83
13. Bahlawane N, Watanaba T, New sol-gel route for the preparation of pure  $\alpha$ -alumina at 950 °C, *J.Am.Ceram.Soc.* 2000, 83(9), 2324-26
14. P.Sakthivel, Alison Christina Fernandez, Joe Jesudurai, Hydrothermal Synthesis of zinc

- oxide-Aluminum oxide nanocomposite, Elixir nanocomposite materials, 50 (2012) 10558-10560*
15. *IARC Monographs on the Evaluation of Carcinogenic Risks to Humans, VOLUME 83, Tobacco Smoke and Involuntary Smoking, LYON, FRANCE 2004*
  16. *Coronary Heart Disease Statistics 2007. Chapter 4: Smoking. British Heart Foundation 2007*
  17. Jaya Lakshmi, M, Venu Gopal, N, Raja, K.P, Mohan Rao, M, Nano SnO<sub>2</sub>-Al<sub>2</sub>O<sub>3</sub> mixed oxide and SnO<sub>2</sub>-Al<sub>2</sub>O<sub>3</sub>-carbon composite oxides as new and novel electrodes for supercapacitor applications, J. power sources, Vol. 158,(2006) 1538-1543p
  18. *Chinh NQ, Gubicza J, Langdon TG. Characteristics of face-centered cubic metals processed by equal-channel angular pressing. J.Mater.Sci. 2007; 42(5): 1594-1605*
  19. *Wells A.F. (1984), Structural Inorganic Chemistry, 5th edition, Oxford Science Publications ISBN 0-19-855370-6*
  20. *Science and Technology of Chemiresistor Gas Sensors By Dinesh K. Aswal, Shiv K. Gupta (2006), Nova Publishers, ISBN 1-60021-514-9*
  21. *Mattias Öberg, Maritta S. Jaakkola, Annette Prüss-Üstün, Christian Schweizer, Alistair Woodward, Second-hand smoke-Assessing the burden of disease at national and local levels, WHO Environmental Burden of Disease Series, No. 18 (2010)*